Desalination and Water Treatment
www.deswater.com

doi:10.5004/dwt.2017.20973

82 (2017) 157–169
July

Comparing cadmium removal efficiency of a magnetized biochar based on orange peel with those of conventional orange peel and unmodified biochar

Mohammad Hossien Salmani[a], Mohammad Miri[a], Mohammad Hassan Ehrampoush[a], Ahmad Alahabadi[b], Ahmad Hosseini-Bandegharaei[b,c,*]

[a]*Department of Environmental Health, Shahid Sadoughi University of Medical Science, Yazd, Iran, Tel. +98 831 4216143, Fax +98 831 4223210, email: MHSN06@yahoo.com (M.H. Salmani), M_miri87@yahoo.com (M. Miri), ehrampoush@ssu.ac.ir (M.H. Ehrampoush)*
[b]*Department of Environmental Health, School of Public Health, Sabzevar University of Medical Sciences, Sabzevar, Iran, Tel. +98 5144419572, Fax +98 5144445648, email: ahmad_health@yahoo.com (A. Alahabadi), ahoseinib@yahoo.com, ahoseinib@iaukashmar.ac.ir (A. Hosseini-Bandegharaei)*
[c]*Department of Engineering, Kashmar Branch, Islamic Azad University, PO Box 161, Kashmar, Iran*

Received 8 May 2016; Accepted 25 May 2017

ABSTRACT

The objective of this study was to investigate the influence of several factors in adsorption of cadmium ions on an advantageous novel low-cost sorbent synthesized from orange peel, nano iron oxide-modified orange peel biochar (IOM-OPB). The adsorption efficiency of IOM-OPB was compared with those of conventional orange peel (OP) and orange peel biochar (OPB). To find the optimum conditions that would give the highest removal efficiency, the effects of several physiochemical factors such as contact time, pH and initial concentration were tested using batch adsorption in a step by step procedure and factorial design. Main effects and interaction effects of three factors were analyzed by using statistical software MINITAB-Version 16. The results indicated that a maximum adsorbent capacity of IOM-OPB was higher than those of OP, OPB. Also, although the type of adsorbent, initial cadmium concentration and pH affect on the removal process, the adsorbent type has the biggest effect on the cadmium adsorption. The results of kinetic, equilibrium and thermodynamic experiments indicated that adsorption process of cadmium onto IOM-OPB is more favorable than onto OP and OPB. Overall, the obtained results showed that IOM-OPB is promising advantageous low-cost adsorbent which can be applied in the real treatment plants.

Keywords: Orange peel; Iron oxide nanoparticle; Cadmium; Adsorption; Biochar

1. Introduction

Excessive release of toxic heavy metals, including cadmium, into the environment is a major concern worldwide due to their harmfulness to each type of life [1–3]. Industries such as mining, refining, electroplating, electronics, alloys manufacturing, batteries, pesticides, etc. severely threaten human lives through discharging various amounts of toxic heavy metal wastewaters to the environment [4–6].

Cadmium is one of the highly toxic heavy metals and cause a number of acute and chronic disorders such as Itai-Itai disease, emphysema, renal damage, hypertension and testicular atrophy [7,8]. Exposing to cadmium at low concentrations has long-term effects on man health and, therefore, it belongs to the chemicals list of priority control pollutants by IARC, WHO and some other agencies [9,10].

The removal of heavy metals from waters and wastewaters in an effective manner is ecologically very important and, from environmental public health point of view, investigating on more simple and efficient techniques for removing heavy metals from industrial wastewaters and

*Corresponding author.

polluted waters is of great scientific value. The conventional technologies which are used for removal of heavy metals from polluted aqueous solutions includes chemical precipitation, solvent extraction, flotation, lime coagulation, ion exchange, reverse osmosis and adsorption [11–16]. The prolific use of some low-cost adsorbents and their chars is relevant to complexing agents existing in their structure, which improve their removal performance towards the interested metal ions [17,18]. In the recent decades, the search for finding low-cost adsorbents that have good binding capacities for heavy metals has been intensified. Agriculture by-products and their chars have found wide uses in the removal of harmful heavy metals from polluted waters and wastewaters, because of their adsorption properties and cost-effectiveness [19–31]. However, the practical use of majority of agriculture by-products is associated with problems like low effectiveness, generation of secondary wastes, and difficulties in separation from wastewater. On the other hand, due to higher chemical stability, porosity, specific surface area and adsorption capacity, the uses of synthesized chars in the full-scale plans are more beneficial than those of low-cost adsorbents originated from agriculture wastes.

Recently, magnetic nano-adsorbents have attracted substantial attention because of its high adsorption efficiency and application feasibility for water and wastewater treatment plans. Modification of solid supports with magnetic nanoparticles has been further successful in the solid–liquid separation problems which are usually encountered with usual adsorbents [17]. Furthermore, nanoiron oxide-modified adsorbents are possibly applied in large-scale industrial wastewater treatment due to their environmentally friendly and easily synthesized characteristics [32–34].

Orange peel (OP), a by-product of the orange juice and soft drink industries, is considered an abundant and inexpensive adsorbent because of the presence of biopolymers, such as polysaccharides, pectin, lignin, hemicelluloses, chlorophyll pigments, and other low hydrocarbons [35,36]. These biopolymers include abundant oxygen-containing functional groups (i.e., –COOH and –OH) and are potentially useful for the efficient uptake of heavy metal ions from aqueous solutions. In this study, due to the aforementioned drawbacks of using agriculture by-products and the advantages of using them in char form, two new biochar adsorbents were synthesized from orange peel (OP), i.e. conventional orange peel biochar (OPB) and nano iron oxide-modified orange peel biochar (IOM/OPB).The adsorption performance of IOM-OPB and OPB towards cadmium ions was compared with that of pristine orange peel (OP; also known as biosorbent). The effects of several operation parameters, such as solution pH, contact time, and initial cadmium concentration, on the removal process of Cd^{2+} ions were investigated and, using experimental design, the influences of factors affecting on the optimization of adsorption process were analyzed.

2. Experimental

2.1. Materials and apparatus

All dilutions throughout this work were performed by highly pure deionized water (Milli-Q Millipore, 18.2 MΩ cm^{-1} resistivity). All chemicals used in this work, *unless* otherwise *specified*, were purchased from Merck (Darmstadt, Germany) and were of AR grade. The stock solution of Cd^{2+} (1000 mg L^{-1}) was prepared by dissolving the appropriate amount of its nitrate salt in deionized water, and all the working solutions at necessary concentrations were prepared by diluting these stock solution. The solutions of 1.0 M HCl or 1.0 M NaOH were utilized for adjusting pH of working solutions.

Fresh orange peels were purchased, washed with distilled water, dried at laboratory temperature (27 ±2°C) for two weeks, grounded in an electrical mill, and sieved to obtain particles in the size range of 0.149–0.250 mm. The particles were divided into three parts. The first part was labeled as OP (orange peel) and used without any further modification or treatment. The second part was introduced into a crucible and pyrolyzed at 400°C for 3 h to prepare OPB (orange peel biochar).The third part was soaked in a solution containing synthesized iron oxide nanoparticles [37] and then washed repeatedly with distillated water. Subsequently, the dried sample was introduced into the crucible and pyrolyzed at 400°C for 3 h to obtain IOM-OPB (iron oxide modified-orange peel biochar).After pyrolysis process, the OPB and IOM-OPB samples were cooled in a desiccator, washed with distillated water, and dried at 105°C for 24 h.

The functional groups on the adsorbent surface were detected using Fourier transform infrared spectroscopy (FTIR; AVATAR 370-FTIR Thermo Nicolet); the adsorbent particles were pelleted for FTIR measurement by mixing with KBr. The field emission scanning electron microscopic (FE-SEM) micrographs were obtained using a VEGA TESCAN instrument, after coating adsorbents surface with gold by a sputter coater instrument (Model SC 7620). The pH of the solutions was measured using a digital pH meter (Corning120 model). The cadmium concentration in solution was determined using an atomic absorption spectrophotometer model AA-20 (Varian, Germany) at a wavelength of 228.8 nm in the standard mode.

2.2. Methods

2.2.1. Design of experiments

To reduce the total number of experiments, experimental design was employed to achieve the optimization conditions, varying initial concentrations and solutions pH as the most important parameters in the investigation of adsorption process. In contrast, other operation parameters were fixed, such as shaker speed of 150 rpm, solid/liquid ratio of 10 g/L, and temperature of 27°C. Furthermore, contact time was firstly optimized, and the optimized value (60 min) was used for the further experiments. Table 1 summarized the characteristics, experimental ranges and levels of factors used in this study.

In order to establish the experimental designs, the Minitab software version 16 was employed, and the main effects and interactions between the tested factors were then thoroughly determined.

2.2.2. Determination of pH_{pzc}

The pH value at the point of zero charge (PZC; pH_{PZC}) was determined using the "drift method". To determine

Table 1
Characteristic and levels of the factors

Factors	Name	Type	Level		
			1	2	3
Ads	Type of adsorbent	Qualitative	OP	OPB	IOM-OPB
pH	pH	Quantitative	3	5	7
C_0	Cd concentration (mg/L)	Quantitative	10	50	100

the values of pH_{pzc} for each adsorbent, six different conical flasks containing 50 mL of 0.01 M NaCl were prepared and their pHs were adjusted in the range of 2–12 and then 0.25 g of the adsorbent was added to these solutions. After shaking for 48 h, the final pH of the solutions was measured by using the digital pH meter. The plot of $pH_{final} - pH_{initial}$ *vs.* $pH_{initial}$ was plotted for each of three adsorbents (OP, OPB and IOM-OPB). The intersection point of $pH_{final} - pH_{initial}$ *vs.* $pH_{initial}$ curve and the bisector provides pH_{PZC}[38].

2.2.3. Adsorption experiments

Batch adsorption experiments of cadmium ions onto the three adsorbents (OP, OPB and IOM-OPB) were carried out at known temperatures and different initial concentrations of Cd^{2+} (10, 50, 100 mg/L) by shaking a series of Erlenmeyers containing 1g of adsorbent and 100 mL of Cd^{2+} solution. Moreover, experiments were carried out at initial pH values ranging from 2 to 7. The equilibrium time was determined by measurement of the removal percent of cadmium at different times ranging from 0 to 180 min, after contacting 1% w/v of adsorbent with 100 ml of 50 mg/L cadmium solution. In each experiment, OP and OPB were separated using a 0.45-μm cellulose filter, while IOM–OPB was magnetically separated from the working solution.

The amount of Cd uptake (q; mg/g) was calculated using the mass balance relation:

$$q = \frac{(C_0 - C_f)V}{m} \quad (1)$$

where C_0 and C_f are initial and final Cd^{2+} concentration (mg/L), respectively; V is the volume of the Cd^{2+} solution (L); and m is the mass of used adsorbent (g).

3. Results and discussion

3.1. Characterization of adsorbent

3.1.1. Determination of point zero charge (pH_{pzc})

The electrical state of the adsorbents surfaces in solutions was characterized by the point of zero charge (PZC). The pH value at which the net (external and internal) surface charge of an adsorbent is zero is defined as pH_{PZC}. In essential, when the pH of a solution ($pH_{solution}$) exceeds the pH_{PZC}, the adsorbent's surface becomes negatively charged because of the deprotonation of oxygen-containing surface groups (i.e., –COOH and –OH), favoring the adsorption of cationic ions (i.e., Cd^{2+} ions) from the solution and vice versa.

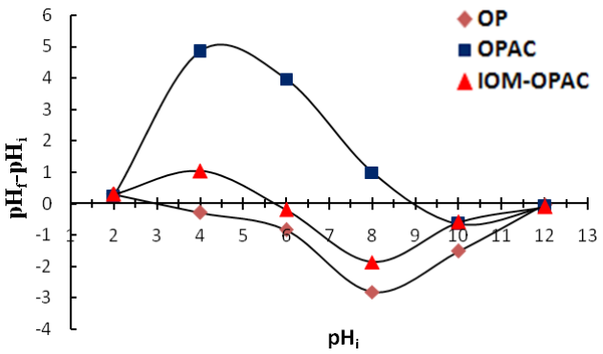

Fig. 1. Plots of $pH_{final} - pH_{initial}$ *vs* $pH_{initial}$ of the studied adsorbents.

Fig. 1 presents the plots of $pH_{final} - pH_{initial}$ *vs.* $pH_{initial}$ for all three adsorbents. According to the plot, the pH_{PZC} values of were as follows: OPB (8.8) > IOM-OPB (5.8) > OP (3.0). Generally, higher PZC values often coincide with a lower densityof oxygen-containing acidic groups on the surface.

3.1.2. FTIR analysis

The decomposition and cracking of a great number of structures present in the precursor during carbonization process as well as the interaction of nano particles with a solid support can be realized by FTIR analysis and finding the shifting, disappearance, and appearance of certain peaks in solid support modified with nano particles, as compared to unmodified solid support spectrum. The characteristic peaks of all three studied adsorbents (OP, OPB and IOM–OPB) can be observed from their FTIR spectra (Fig. 2). The main differences between OP, OPB, and IOM-OPB, which are seen at the first glance of their spectrum, can be contributed to the carbonization process. In comparison to the OP spectrum, both OPB and IOM-OPB spectra showed lack of the absorption peak at 2929 cm^{-1} and the broad intense band at 4424 cm^{-1} which can be, respectively, contributed to the stretching vibrations of aliphatic C–H bonds and the O–H stretching vibrations of carboxylic acids, as in pectin, cellulose and lign in [39,40]. Also, there is a missing small peak at 1745 cm^{-1} in both OPB and IOM-OPB spectra, which may be related to the decomposition of carboxylic groups during the carbonization process. Moreover, the lack of peaks in the fingerprint region of both OPB and IOM-OPB spectra can be contributed to the decomposition and cracking of a great number of structures present in the orange peel. Also, notably, the appearance of new peak observed at approximately 640 cm^{-1} in the IOM–OPB spectrum the existence of

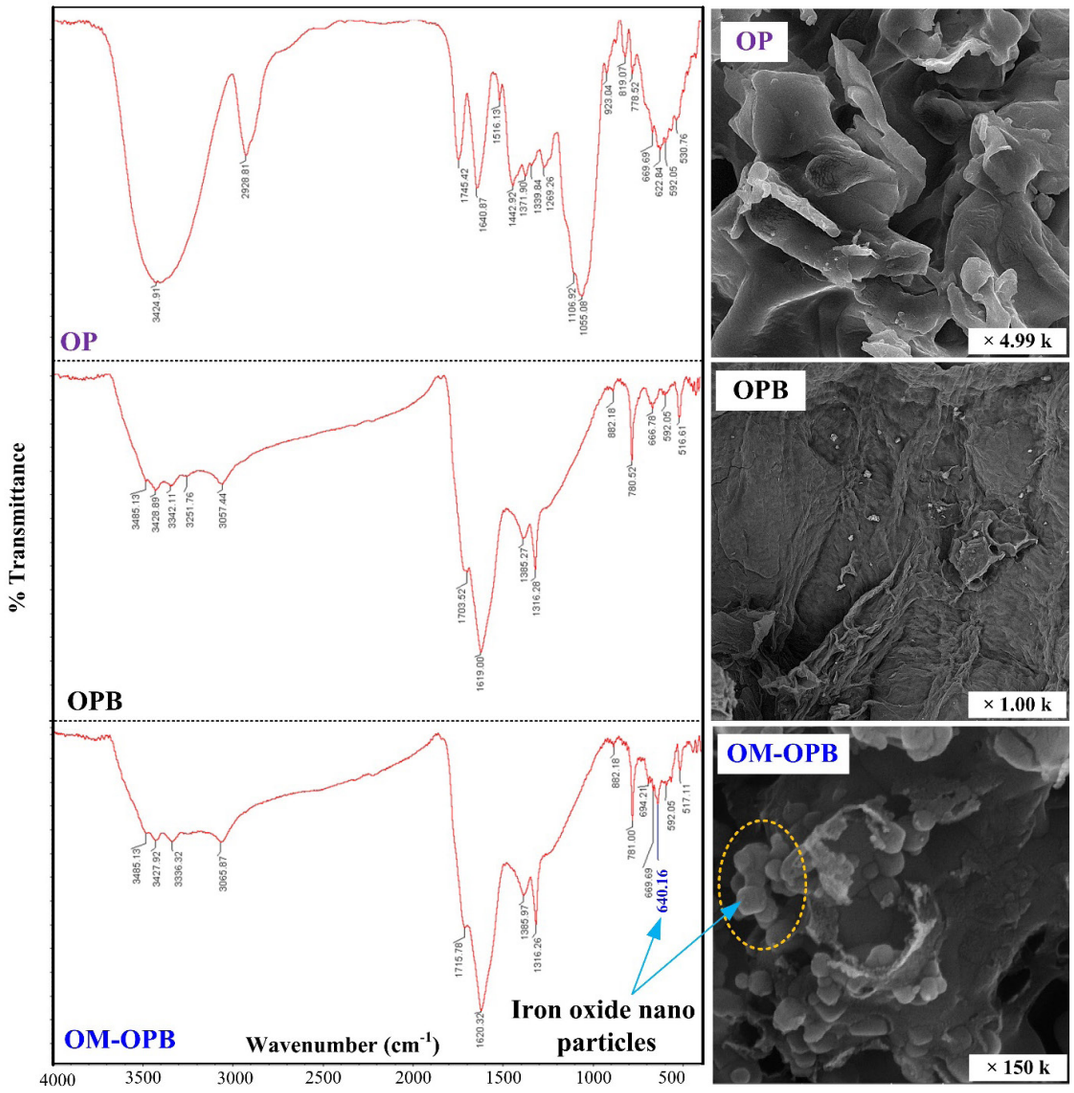

Fig. 2. FT-IR spectra and FE-SEM micrographs of the studied adsorbents.

(Fe–O) iron oxide in its surface [34]. However, more precise comparison of FTIR spectra of OPB and IOM–OPB reveals significant band shifting from 3057.44 cm^{-1} and 1703.52 cm^{-1} on OPB to, respectively, 3065.87 cm^{-1} and 1715.78 cm^{-1} on IOM–OPB, corresponding to $–CH_2$ and –C=O stretching, indicating the effective interaction of iron oxide nano particles and carbon solid support to form stable IOM-OPB adsorbent.

3.1.3. FE-SEM micrographs

The morphology of OP, OPB, and IOM-OPB was observed in Fig. 2. As shown in FE-SEM micrographs, the OP, OPB, and IOM-OPB samples had low porosities and fairly rough surfaces, which often coincide with their low textural properties. Therefore, the Cd adsorption efficiency might be mainly attributed to their high surface functionalities. As expected, the iron oxide nano particles can be observed in the surface morphology of IOM-OPB, suggesting that iron oxide was successfully modified into the surface of OP. Furthermore, the IOM-OPB micrograph also demonstrated that the iron oxide nano particles were fine and their size was smaller than 55 nm, without significant agglomeration of particles.

3.2. Effect of factorial design

Design of experiments allows the simultaneous study of several factors which may have effects on an optimization of a particular process. The factorial design determines which factors have important effects on a response as well as how the effect of one factor varies with the known lev-

els of the other factors. The optimization of all these variables using univariate procedure is time-consuming, since any variable is optimized by varying one factor and fixing the others at known amounts. The main drawback of this procedure is that the best conditions could not be obtained because the interactions among all the factors are disregarded. This disadvantage can be overcome by statistical design of experiments, and achieving the best optimization of system conditions. In addition, statistical design of experiments would lead to the reduced number of experiments and obtaining better response [41].

In a full factorial experimental design, responses are measured at all combinations of the experimental factor levels. The combination of factor levels represents the conditions at which responses will be measured [42]. In this work, a 3^3 full factorial design was employed and related experiments were carried out. The variables effects and their interactions were measured by performing a set of 27 experiments containing 3 levels of initial concentration and 3 levels of pH for 3 adsorbent. Table 2 represents the full experimental design with sorption capacities of the studied sorbents.

The main effects of the significant factors affecting the adsorption capacity of adsorbents were determined by performing an analysis of variance (ANOVA). Whereas in this study 3 levels of factors were estimated, each ANOVA main effect had two degree of freedom and interactions effects had their product. Table 3 reports the sum of squares, degree of freedom, mean square, and F and P-value in this study.

All of the main factors and their interactions were significant at 95% confidence level. From the Table 3, the C_0 effect present the high statistical significant (F-value = 421.6 and P-value = 0.001). Also, the significance of adsorbent type effect is of the second order. By comparison, pH has almost the low effect on adsorption capacity of adsorbents.

The regression coefficients, the associated standard errors and effects are reported in Table 4 and, also, the significance of each coefficient has been determined by T-values and P-values which are listed in this table. The larger the magnitude of T-values and smaller the P-values have more significant in the corresponding coefficient [43].

It should be denoted that, when the effect of a factor is positive, an increase in the value of the response is observed by increasing the factor value from low to high levels. In contrast, when the effect of a factor is negative, a reduction in adsorption capacity occurs in its high levels.

According to Table 4, it seems that the type of adsorbent was the most important variable of the adsorption capacity, since its coefficient was the largest one (3.0411). The changes in the adsorbent type from OP (indicated by level 1) to IOM-OPB (indicated by level 3) increased the adsorption capacity about 9.12%. The initial concentration and pH had the small effects on adsorption capacity. The results showed that an increase in the cadmium concentration from 10 to 100 mg/L increased adsorption capacity by 2.43%. Furthermore, an increase in the solution pH from 3 to 7 alone increased the adsorption capacity by 0.46%

Table 2
Design of experiments and results for sorption capacity

pH	OP			OPB			IOM-OPB		
	10	50	100	10	50	100	10	50	100
					Sorption	Capacity			
3	0.83±0.21	3.97±0.15	6.43±0.20	0.69±0.01	2.82±0.02	4.60±0.01	0.48±0.25	2.57±0.03	5.96±0.12
5	0.72±0.01	3.26±0.01	4.92±0.02	0.91±0.01	4.31±0.01	7.32±0.08	0.72±0.03	4.27±0.02	8.91±0.02
7	0.64±0.02	3.42±1.07	4.23±0.01	0.80±0.02	3.68±0.01	7.02±1.09	0.87±0.03	4.50±0.05	9.26±0.06

Table 3
Analysis of variance- Tests of between-subjects effects

Factors	Statistic				
	Sum of squares	D.F.	Mean square	F	P-value
Corrected Model	517.502*	26	19.904	39.510	0.001
Intercept	1102.904	1	1102.904	2.189E3	0.002
pH	5.562	2	2.781	5.520	0.007
C_0	424.785	2	212.393	421.606	0.001
Ads	19.297	2	9.648	19.152	0.001
pH*C_0	8.834	4	2.208	4.384	0.004
pH*Ads	19.121	4	4.780	9.489	0.002
C_0*Ads	19.108	4	4.777	9.483	0.001
pH*C_0*Ads	20.795	8	2.599	5.160	0.001
Error	27.204	54	0.504		
Total	1647.610	81			

*R^2 = 0.950 (Adjusted R^2 = 0.926)

Table 4
Estimated regression coefficients for adsorption capacity

Terms	Statistic			
	Coefficient	SE Coefficient	T	P-value
Intercept	2.1424	1.047	2.045	0.045
pH	0.2281	0.602	0.379	0.706
C_0	0.8126	0.602	1.350	0.181
Ads	–3.0411	0.602	-5.052	0.000
pH*pH	–0.5009	0.133	-3.752	0.000
C_0*C_0	0.0396	0.133	0.297	0.767
Ads*Ads	0.1424	0.133	1.067	0.290
pH*C_0	0.2108	0.0944	2.233	0.029
C_0*Ads	0.7169	0.0944	7.595	0.000
pH *Ads	0.7983	0.0944	8.457	0.000

R^2 = 0.956 (Adjusted R^2 = 0.951)

The main effects of each parameter on the adsorption capacity can be seen in Fig. 3 in which plots represent the results of regression analysis. It can be seen from Fig. 3 that three studied parameters have a positive influence upon adsorption process efficiency, which is in a strong correlation with the results obtained from the adsorption studies.

The effect of a factor in adsorption appears with the change in level of that factor and, when it changes from low level to high level, the larger verticality in lines means the larger changes in adsorption capacity [44]. In Fig. 3, it can be seen that the larger verticality of line is of the parameter C_o, and so it has the larger effect on the adsorption capacity. The interaction effects of each parameter on the adsorption capacity are shown in Fig. 3 in which all parameters have shown a positive influence upon the adsorption efficiency of process. A great deviation from the parallelism put in evidence a strong interaction among control factors. Fig. 3 shows the following significance interactions: adsorbent type and pH, adsorbent type and initial concentration for adsorption capacity, respectively. According to the ANOVA values, interaction of adsorbent type and initial concentration is the most significant interaction. The other important interaction is pH and adsorbent type. It was observed (Fig. 3) that the effect of C_0 was more noticeable when the adsorbent was modified with iron oxide (high level) but the effect of pH was not so high when the adsorbent type changes. On the contrary, the effects of pH and initial concentration were not important at lower adsorbent level of OP.

The response surface to estimate the adsorption capacity of Cd^{2+} over independent variables of pH and initial metal concentration is depicted in Fig. 4.

The points giving the maximum adsorption capacity of OP, OPB and IOM-OPB were, respectively, found to be at 100 mg/L initial cadmium concentration and pH of 3, 5 and 7. The poor adsorption of Cd^{2+} in the low pH could be due to competition with the H^+ ions for metal binding sites on the adsorbents, while the increase in pH favors metal adsorption, mainly because of negatively charged groups. However, from the other hand, complexing agents existing in the structure of adsorbents can strongly interact with

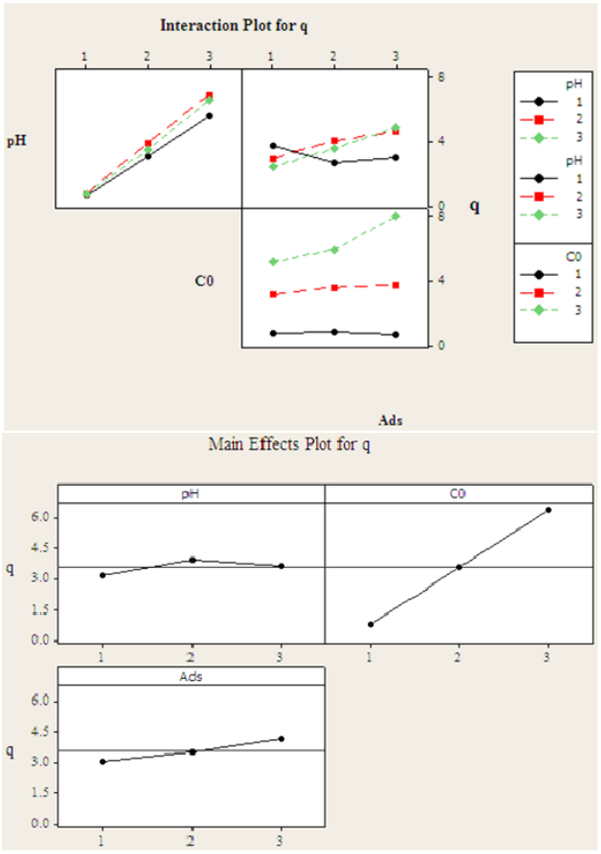

Fig. 3. The main effects of each parameter on the adsorption capacity.

metal ions at desired pHs which may be either higher or lower than pH_{PZC}.

3.3. Optimization of adsorption process

The sorption process depends on various factors such as pH, sorbent dosage, adsorbate concentration in solution, sorbent type, temperature, and agitation time. In this study, the factors screened were initial cadmium concentration, pH and contact time for all three adsorbents. The experiments were carried out in a batch process and cadmium removal was estimated in each step.

3.3.1. Effect of contact time

A time required for adsorbent capacity to reach a constant value during the adsorption process was defined as equilibrium time. Fig. 5 shows the removal percent of cadmium against contact time. The results represented in Fig. 5 shows that the removal of cadmium ions increases with time and attains to saturation state in about 60 min and, basically, the removal of cadmium ions for all three adsorbents is rapid.

As can be seen from this figure, respectively in the case of OP, OPB and IOM-OPB, 48.5, 55.6 and 51.5% (2.41, 2.78

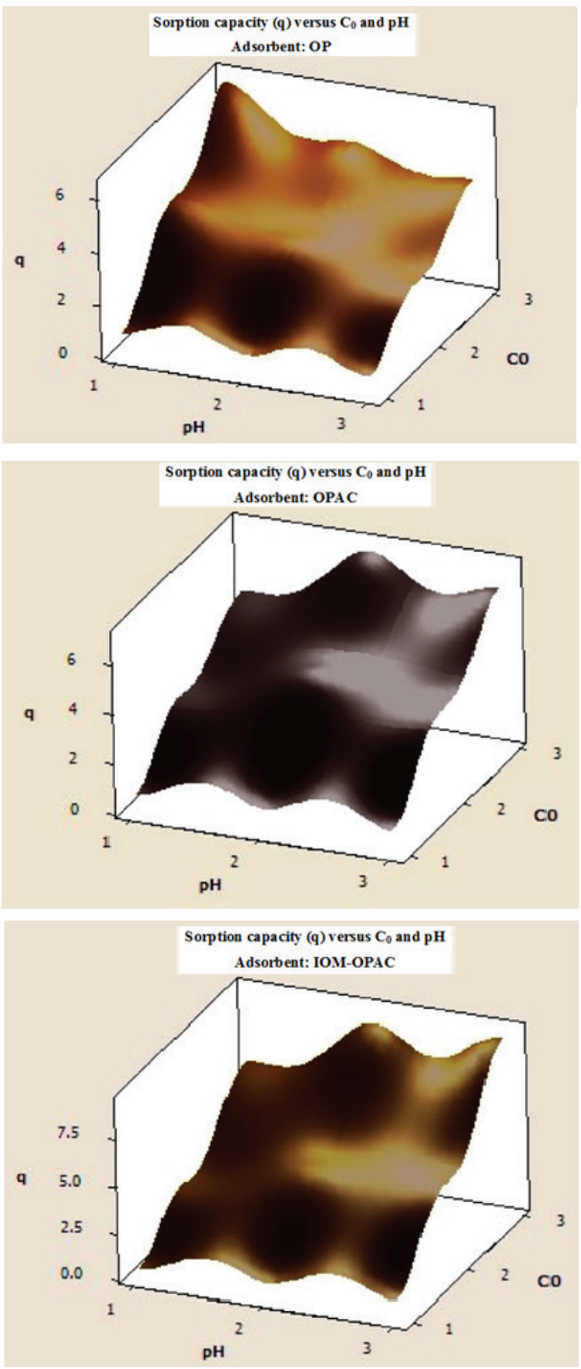

Fig. 4. The response surface to estimate the adsorption capacity of cadmium over independent variables of pH and initial metal concentration.

and 2.57 mg/g) of cadmium were adsorbed in the first 30 min. From 30 to 60 min the adsorption was gradually increased from 48.5, 55.6 and 51.5% to 68.1, 86.2 and 89.9% for OP, OPB and IOM-OPB, respectively. Beyond 60 min, the removal percent of cadmium was marginal, indicating the attainment of equilibrium conditions. It can be mentioned

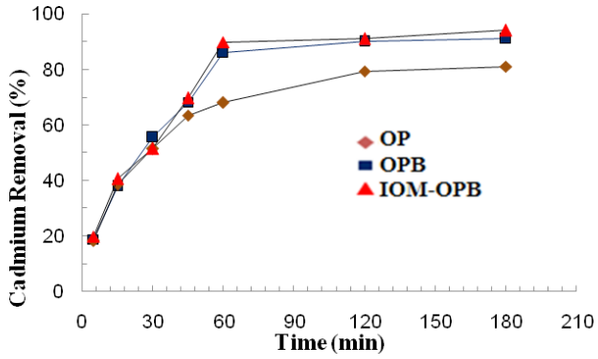

Fig. 5. Removal percentage of cadmium against contact time at optimum pH values (Volume, 100 mL; initial concentration, 100 mg L^{-1}; adsorbent dose, 1.0 g; temperature, 27°C; agitation speed, 150 rpm).

that the rate of metal removal was fast in the beginning due to the availability of a larger surface area of the adsorbent for the cadmium ions. As time increases, more amount of cadmium settles onto the adsorbent surface which results in decreased availability of surface area for cadmium ions, and diminishing the adsorption rate. As it has been extensively reported in literature, this usually cause a two-stage sorption mechanism in which the first step is fast, predominant and quantitatively significant and the second step is slower and quantitatively insignificant [45].

3.3.2. *Effect of the initial aqueous solution pH*

The effect of the solution pH on the adsorption process can be explained on the basis of charge of adsorbent which depends on the value of pH_{pzc}. Dissolved elements in waters may be present in many different forms such as hydrated species, and chelated with inorganic carbonate, hydroxide, chloride, sulfate, or organic compounds. Depending on the solution pH, dissolved cadmium in waters may be present in many different forms such as Cd^{2+}, $CdOH^{+}$, $Cd(OH)_2$, $Cd(OH)_3^-$ and $Cd(OH)_4^{2-}$ [46]. In the present study, cadmium adsorption data were obtained in the pH range of 3 to 7. The effect of aqueous solution pH on cadmium removal was shown in Fig. 6 for three adsorbents. By increasing pH from 3 to 7, the cadmium removal was decreased from 77.5% to 48.5% for OP, while it was increased from 51.4% to 89.9% for IOM-OPB. Also, as can be noted, the removal of cadmium by OPB was increased from 56.4% to 83.2% by increasing pH from 3 to 5 and beyond pH 5, the cadmium removal was marginally decreased (73.4% in pH 7).

The pH affects not only the surface change of the adsorbent but also the degree of ionization and the species of adsorbate in aqueous solution [47]. Therefore, the effect of pH can be explained in terms of surface charge and metal ions species in the solution. In general, when the pH of adsorbing solution is increased, there is a corresponding of decrease in the H^+ ions and deporotonation of the sorbent surface, reciprocally. This creates more negative charge on the sorbent surface, which favors adsorption of positively charge species as a result of less repulsion between the cations and active sites on the surface [48]. On the other hand,

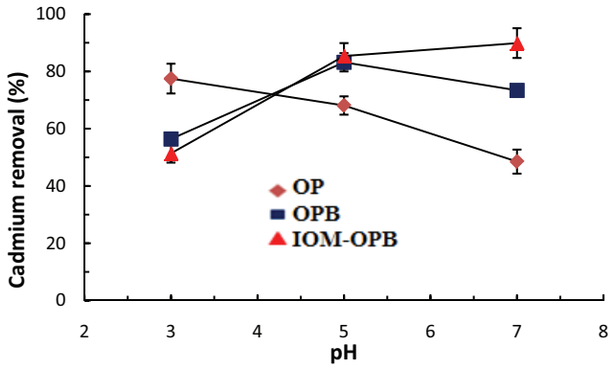

Fig. 6. Effect of aqueous solution pH on cadmium removal (Volume, 100 mL; adsorbent dose, 1.0 g; initial concentration, 100 mg L^{-1}; contact time, 60 min; temperature, 27°C; agitation speed, 150 rpm).

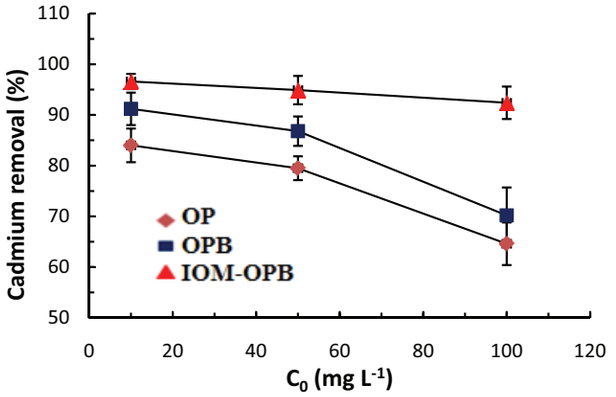

Fig. 7. Effect of cadmium initial concentration on the % removal in the optimum pH values (Volume, 100 mL; adsorbent dose, 1.0 g; contact time, 60 min; temperature, 27°C; agitation speed, 150 rpm).

low pH depresses adsorption of cadmium, due to competition with H^+ ions for appropriate sites on the adsorbent surface. However, with increasing pH, this competition weakens and Cd^{2+} ions replace H^+ ions bound to the surface functional groups such as OH on the adsorbent. Also it should be mentioned that complexing agents existing in their structure of some low-cost adsorbents and their chars can strongly interact with metal ions at desired pHs which may be either higher or lower than pH_{PZC}.

It should be noted that the optimum pH of adsorption process was equal or lower than pH_{pzc} values obtained for all three adsorbents. Therefore, adsorption of Cd^{2+} ions by OP, OPB and IOM-OPB indicated that the cadmium ion adsorption proceeds via factors such as chelating with functional groups.

3.3.3. Effect of cadmium initial concentration

Fig. 7 represents the effects of cadmium initial concentrations of 10, 50 and 100 mg/L on the percentage of Cd^{2+} removed from aqueous solutions. Clearly, the percentage of cadmium removal decreased from 84.0% to 64.5% for OP, 91.2% to 70.2% for OPB, and 96.8% to 92.4% for IOM-OPB-with an increase in C_0 from 10 to 100 mg/L.

High adsorption of Cd^{2+} in the first stage involves adsorption sites with high energy and thereafter adsorption in the low energy sites begins, resulting in a decrease in removal percentages at the higher concentrations. Moreover, the higher capability of iron oxide modified-adsorbent (IOM-OPB) for cadmium adsorption can be attributed to the increase in the number of active sites in cause of modification.

3.4. Adsorption isotherms

After a necessary period of contact time, equilibrium state for an adsorption system is achieved and, in this state, the amount of adsorbate adsorbed onto the adsorbent surface is introduced as the equilibrium capacity (q_e) which is a function of equilibrium concentration (C_e) and equilibrium temperature (T), i.e. q_e (C_e, T) [49]. Since the investigation of the characteristics of adsorption isotherm is of great importance in any adsorption system design, study of adsorption isotherms for all three adsorbents was performed by utilizing the data obtained from the investigation of effect of initial concentration. Two well-known adsorption isotherms viz. Langmuir [50] and Freundlich [51] were used to fit the experimental data and describe the adsorption behavior obeyed in cadmium adsorption by the studied adsorbents.

The Langmuir isotherm model assumes the adsorption proceeds via a homogenous process and usually is used to calculate the maximum adsorption capacity corresponding to the complete monolayer coverage without any interaction between the adsorbed pollutant molecules. The linear form of Langmuir can be represented by the following relation:

$$\frac{C_e}{q_e} = \frac{C_e}{q_{\max}} + \frac{1}{bq_{\max}} \tag{2}$$

where C_e (mg L^{-1}) is the equilibrium concentration of adsorbate, q_e (mg g^{-1}) is the adsorption capacity of the adsorbent at the equilibrium, q_{max} (mg g^{-1}) is the maximum capacity, and b (L mg^{-1}) is the Langmuir constant related to the affinity of adsorption sites.

The Freundlich isotherm assumes that the adsorption proceeds via a non-ideal, reversible and multilayer heterogeneous process. The linear form of Freundlich relation can be presented by the following equation:

$$\log q_e = \log K_f + \frac{1}{n}\log C_e \tag{3}$$

where C_e (mg L^{-1}) is the equilibrium concentration, K_F ($mg^{1-(1/n)}.L^{1/n}.g^{-1}$) is roughly an indicator for the adsorption capacity and n is related to the adsorption intensity which has a numerical value and varies with heterogeneity. The magnitude of n for a favorable adsorption is greater than unity.

The linear plots of aforementioned isotherm models for adsorption of cadmium onto OP, OPB and IOM-OPB surfaces are shown in Fig. 8, and the calculated parameters from this plots are reported in Table 5. As can be seen from the results, Langmuir model with higher correlation coefficients (R^2) is assumed to be obeyed by adsorption of

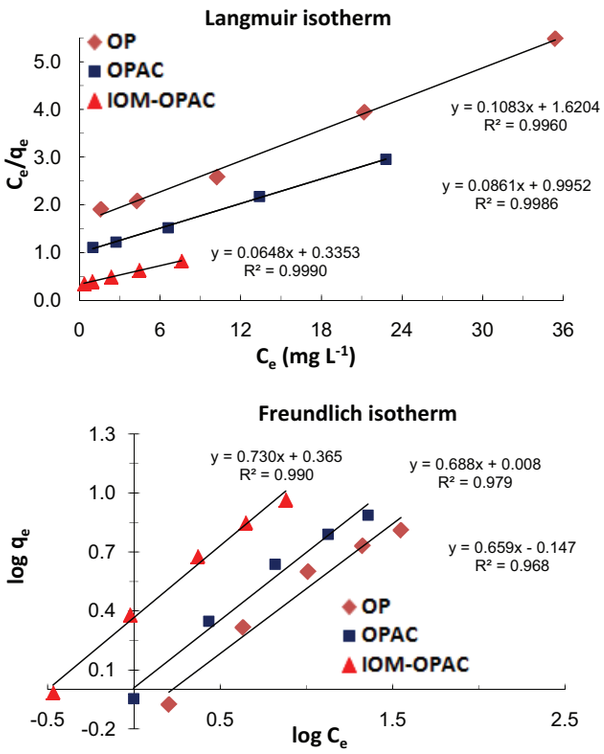

Fig. 8. Linear plots of Langmuir and Freundlich isotherms for cadmium adsorption by the studied adsorbents (T = 27°C).

Table 5
The isotherm information of cadmium adsorption onto the studied adsorbents

Isotherm	Parameters	Magnitude		
		OP	OPB	IOM-OPB
Langmuir	R^2	0.9960	0.9986	0.9990
	b (L·mg^{-1})	0.067	0.086	0.193
	q_{max} (mg·g^{-1})	9.234	11.614	15.432
Freundlich	R^2	0.9683	0.9793	0.9901
	n	1.516	1.452	1.368
	K_F (mg$^{1-(1/n)}$·L$^{1/n}$·g^{-1})	0.712	1.020	2.321

cadmium onto all three adsorbents, giving the maximum adsorption capacities (q_{max} values) with the order of IOM-OPB > OPB > OP which is in agreement with the results obtained from the other studies. These results indicate that the adsorption of cadmium onto all the studied adsorbents is monolayer and the adsorption processes occur at energetically equivalent adsorption sites.

3.5. Adsorption kinetics

The kinetic properties of an adsorption process gain insight on its physical chemistry and selecting the optimum conditions for the design of a full scale adsorption system

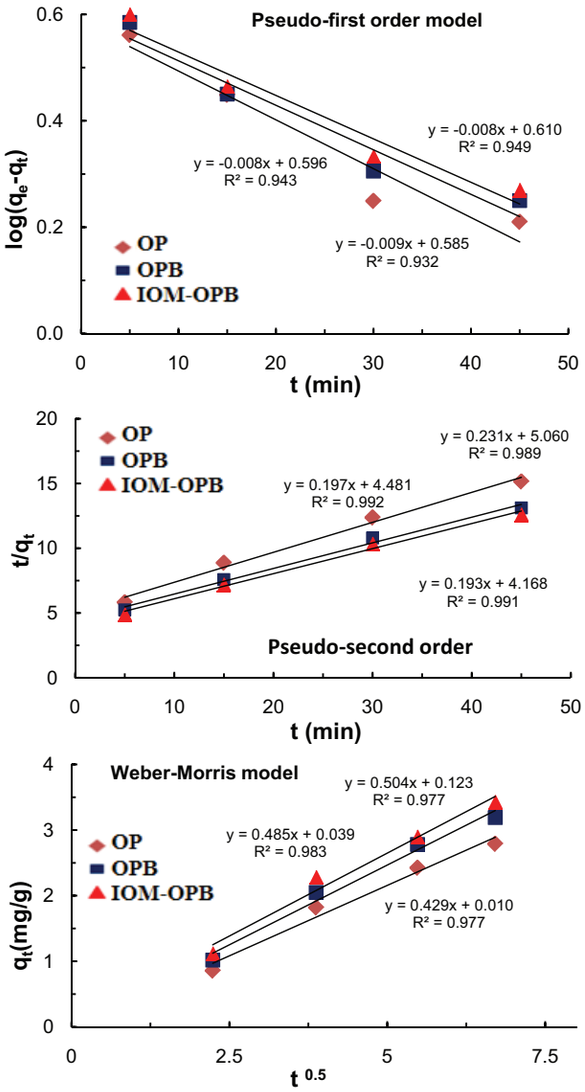

Fig. 9: Linear plots of different kinetic models for cadmium adsorption by the studied adsorbents (T=27 °C).

[6]. Therefore, the adsorption data from the contact time of 5 to 45 min, reported in Fig. 5, were fitted on several kinetic models and the results were discussed below.

The linear form for pseudo-first order model can be given as follows [52]:

$$\log(q_e - q_t) = \log q_e - \frac{k_1}{2.303} t \quad (4)$$

where q_e and q_t are the amounts of adsorbate adsorbed (mg g^{-1}) at equilibrium and at time 't (min)', respectively, t (min) is the time and k_1 is the rate constant of pseudo-first order adsorption (min^{-1}). Values of k_1 and q_e for each adsorbent can be obtained from the slope and intercept of the linear plots of log ($q_e - q_t$) vs. t which are showed in Fig. 9.

The pseudo-second order kinetic model is based on equilibrium adsorption and can be given by the following linear relation [53]:

$$\frac{t}{q_t} = \frac{1}{k_2 q_e^2} + \frac{t}{q_e} \tag{5}$$

where k_2 (g mg^{-1} min^{-1}) is the pseudo-second order rate constant, t (min) is the time, q_e (mg g^{-1}) is the amount of adsorbate adsorbed at equilibrium and q_t (mg g^{-1}) is the amount of adsorbate adsorbed at any instant of time t (min). The linear plots of pseudo second order model is given in Fig. 9 from which constant k_2 and q_e for each adsorbent can be calculated from the slopes and the intercepts of the plots.

Intra-particle diffusion model is commonly represented by Weber and Morris equation [54]:

$$q_t = k_{id} t^{0.5} + I \tag{6}$$

where q_t (mg g^{-1}) is the amount of adsorbate adsorbed at time 't', k_{id} (mg g^{-1} min$^{-0.5}$) is the rate constant of pore diffusion, t (min) is the time and I is constant. When diffusion into the pores of adsorbent is the rate-controlling step, the plot of q_t against $t^{1/2}$ give a straight line with an intercept equal to I value which is proportional to the boundary layer. The values of intra-particle constants for each adsorbent can be obtained from the slope and intercept of the plots of q_t against $t^{1/2}$ which are given in Fig. 9.

Table 6 shows the calculated kinetic parameters for adsorption of cadmium onto OP, OPB and IOM-OPB at initial concentration 50 mg/L. It can be observed that, for all three adsorbents, the correlation coefficients obtained for pseudo-second order model are higher than the other models. Also, the calculated values of q_e by using pseudo-second order rate equation and the experimental values reported in Table 6 are close to each other as compared to the values obtained for the other kinetic models. These results indicate that, for all studied adsorbents, the adsorption kinetics for the adsorption of cadmium is best described by pseudo-second order rate equation, indicating that the interaction between the cadmium ions and the functional groups existing in the surface of adsorbents is the rate-controlling step. The results also showed that k_2 values increased in the order of IOM-OPB > OPB > OP which implies that the adsorption process of cadmium on the IOM-OPB is kinetically more favorable than the other adsorbents.

3.6. Thermodynamic studies

Evaluation of energetic changes during the adsorption process is of great importance for assessing the feasibility and spontaneity of the adsorption process and practical application of the adsorption system. Equilibrium results provide an accurate basis for calculating a correct equilibrium constant, for using in the van't Hoff equation and calculating the thermodynamic parameters [55–57]. Therefore, thermodynamic studies were carried by calculating the constant $55.5b_M$ from the data obtained from equilibrium experiments at 293, 300 and 308 K and substituting them in van't Hoff equation [55–59]:

$$\ln(55.5 b_M) = \frac{\Delta S}{R} - \frac{\Delta H}{RT} \tag{7}$$

where the gas constant R is defined by 8.3145 J mol^{-1} K^{-1}, 55.5 is the number of moles of water per liter of solution, b_M (L mol^{-1}) is the Langmuir constant, T is the temperature of the solution in Kelvin, ΔH (J mol^{-1}) is enthalpy and ΔS (J mol^{-1} K^{-1}) is the entropy change during the adsorption process. Therefore, the values of Langmuir constant (b_M) were calculated at the different temperatures and, then, ΔH (J mol^{-1}) and ΔS (J mol^{-1} K^{-1}) for the adsorption of cadmium onto all the studied adsorbents were calculated from the slop and intercept of plots of $\ln 55.5 b_M$ vs. $1/T$, as shown in Fig. 10.

The free energy changes (ΔG, J mol^{-1}) at different constant temperatures (K) are related to the heat of adsorption, ΔH (J mol^{-1}), and entropy change, ΔS (J mol^{-1} K^{-1}), and can be calculated from the following equation:

$$\Delta G = \Delta H - T\Delta S \tag{8}$$

The thermodynamic parameters were calculated for the removal of cadmium ion by all three adsorbents and listed in Table 7. Since the values obtained for ΔH are positive,

Table 6
Kinetic parameters of different models for cadmium adsorption onto the studied adsorbents

Model	Parameter	Magnitude		
		OP	OPB	IOM-OPB
Pseudo-first-order	k_1 (min^{-1})	2.11E-02	1.93E-02	1.89E-02
	$q_{e\text{-}mod}$ (mg g^{-1})	3.878	3.947	4.079
	R^2	0.9326	0.9434	0.9499
Pseudo-second order	K_2 (g mg^{-1} min^{-1})	1.06E-03	8.74E-03	8.98E-04
	$q_{e\text{-}mod}$ (mg g^{-1})	4.321	5.053	5.168
	R^2	0.9897	0.9922	0.9919
Weber-Morris	k_{ip} (mg g^{-1} min$^{-1/2}$)	0.429	0.486	0.505
	I	1.00E-02	3.91E-02	1.24E-01
	R^2	0.9774	0.9831	0.9774
	$q_{e\text{-}exp}$ (mg g^{-1})	4.06	4.56	4.71

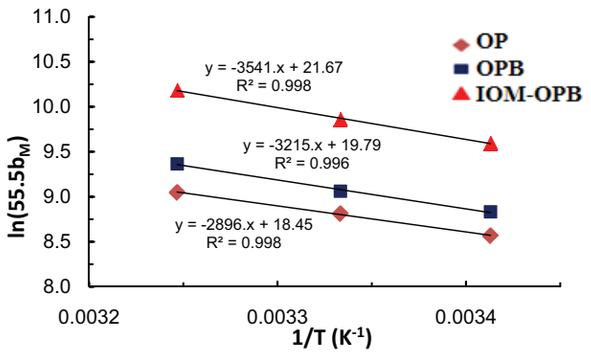

Fig. 10. Thermodynamic plots for cadmium removal by the studied adsorbents.

Table 7
Thermodynamic parameters for the adsorption of cadmium by the studied adsorbents as a function of temperature

Adsorbent	Temprature (K)	$\Delta G°$ (kJ·mol^{-1})	$\Delta H°$ (kJ·mol^{-1})	$\Delta S°$ (J·mol^{-1}·K^{-1})
	293	–23.378		
IOM-OPB	300	–24.597	29.447	180.239
	308	–26.081		
	293	–21.515		
OPB	300	–22.601	26.737	164.609
	308	–23.983		
	293	–20.867		
OP	300	–21.978	24.081	153.443
	308	–23.169		

the adsorption of cadmium onto the surface of all adsorbents is of endothermic nature. The more negative ΔG values obtained for IOM-OPB indicate the more feasibility and spontaneity of cadmium adsorption onto the surface of IOM-OPB, as compared to the two other adsorbents.

3.7. Removal of cadmium from a synthetic water sample

The performances of the studied adsorbents in the presence of some cations and anions was investigated using a synthetic water sample with the following composition (mg L^{-1}): Fe(III) 5.0, Al(III) 2.0, Ni(II) 5.0, Cu(II) 5.0, Mn(II) 5.0, Ca(II) 5.0, Mg(II) 5.0, $(PO_4)^{3-}$ 2.0, and $(SO_4)^{2-}$ 5.0. For this purpose, instead of distilled water, cadmium solution with the concentration of 10 mg/L was prepared by using the above synthetic water sample. Then, 100-mL portions of the prepared solution were contacted with 1.0 g of each adsorbent at the optimum pH and, after equilibration, the residual concentrations of cadmium in the solutions were determined. The results showed that, by using the above synthetic water instead of distilled water, the removal percentage of cadmium was decreased from 84.0, 91.2 and 96.8 % to 69.1, 84.4 and 92.5 % for OP, OPB and IOM-OPB, respectively. These results showed that, in the case of IOM-OPB, applying synthetic water causes the smallest decrease in the removal percentage of cadmium and, therefore, using IOM-OPB in the real treatment plants can bring about a better performance than OP and OPB. Also it should be mentioned that higher removal percentages can be easily reachable by higher adsorbent dosages.

4. Conclusion

This work shows that iron oxide-modified orange peel biochar (IOM-OPB) could find application as adsorbent for the removal of cadmium ions from waters and wastewaters, and its performance is better than those of conventional orange peel (OP) and orange peel biochar (OPB). To reduce the total number of experiments, firstly the optimal process parameters were indicated by preliminary batch studies and then the results were demonstrated by factorial design. The following key conclusions can be mentioned from the obtained results:

1. IOM-OPB can be easily prepared by co-precipitation of orange peel with iron oxide nonomaterials and its carbonization.
2. Factorial design results showed that, compared to the other factors studied, the adsorbent type has the most significant effect on adsorption efficiency, and the order of adsorption capacities for cadmium ion were OP<OPB<IOM-OPB.
3. The adsorption isotherm of cadmium was better described by Langmuir model for all three adsorbents, and the Langmuir monolayer saturation capacities (q_{max}) of OP, OPB and IOM-OPB at ambient temperature (300 K) were 9.234, 11.614 and 15.432 mg g^{-1}, respectively, indicating the higher adsorption capacity of IOM-OPB compared to OP and OPB adsorbents.
4. The kinetic studies showed that pseudo-second order model was more successful for describing the adsorption kinetic of cadmium on all three adsorbents, and k_2 value obtained for IOM-OPB was higher than those of OP and OPB.
5. Thermodynamic studies indicated the more feasibility, spontaneity and favorability of cadmium adsorption onto IOM-OPB, compared to OP and OPB.
6. Since, in addition to higher adsorption capacity, higher kinetic constant and more feasibility in cadmium adsorption, the developed IOM-OPB has additional benefits like easy preparation, fast separation, absence of secondary pollutants, environmental-friendliness, it is a promising advanced adsorbent for water and wastewater treatment plants.

Acknowledgement

This work was financially supported by central research councils of Shahid Sadoughi University and Sabzevar University of Medical Sciences, Iran.

References

[1] A. Sigel, H. Sigel, R.K.O. Sigel, Cadmium: From Toxicity to Essentiality, Springer, Dordrecht, 2013.

[2] A. Alahabadi, M.H. Ehrampoush, M. Miri, H. Ebrahimi Aval, S. Yousefzadeh, H.R. Ghaffari, E. Ahmadi, P. Talebi, Z. Abaszadeh Fathabadi, F. Babai, A. Nikoonahad, K. Sharafi, A. Hosseini-Bandegharaei, A comparative study on capability of different tree species in accumulating heavy metals from soil and ambient air, Chemosphere, 172 (2017) 459–467.

[3] A. Rastegar, A. Alahabadi, A. Esrafili, Z. Rezai, A. Hosseini-Bandegharaei, S. Nazari, Application of supramolecular solvent-based dispersive liquid–liquid microextraction for trace monitoring of lead in food samples, Anal. Methods, 8 (2016) 5533–5539.

[4] L. Järup, Hazards of heavy metal contamination, Br. Med. Bull., 68 (2003) 167–182.

[5] M. de Lourdes Llovera-Hernández, A. Álvarez-Gallegos, J.A. Hernández, S. Silva-Martínez, Cadmium removal from dilute aqueous solutions under galvanostatic mode in a flow-through cell, Desal. Water Treat., 57 (2016) 22809–22817.

[6] A. Hosseini-Bandegharaei, R. Khamirchi, R. Hekmat-Shoar, A. Rahmani-Sani, A. Rastegar, Z. Pajohankia, E. Fattahi, Sorption efficiency of three novel extractant-impregnated resins containing vesuvin towards Pb(II) ion: Effect of nitrate and amine functionalization of resin backbone, Colloids Surf. A Physicochem. Eng. Asp., 504 (2016) 62–74.

[7] M. Jaishankar, T. Tseten, N. Anbalagan, B.B. Mathew, K.N. Beeregowda, Toxicity, mechanism and health effects of some heavy metals, Interdiscip Toxicol., 7 (2014) 60–72.

[8] L. Friberg, C.G. Elinder, T. Kjellström, G. Nordberg, Cadmium and health: a toxicological and epidemiological appraisal vol 1. CRC press Boca Raton, FL, 1986.

[9] G. Kazantzis, Cadmium in the human environment: Toxicity and carcinogenicity, Occup. Environ. Med., 51 (1994) 720–721.

[10] S. Satarug, S.H. Garrett, M. Ann Sens, D.A. Sens, Cadmium, environmental exposure, and Health outcomes, Environ. Health. Perspect., 118 (2010) 182–190.

[11] I. Ali, V. Gupta, Advances in water treatment by adsorption technology, Nat. protoc., 1 (2006) 2661–2667.

[12] M.H. Salmani, M. Davoodi, M.H. Ehrampoush, M.T. Ghaneian, M.H. Fallahzadah, Removal of cadmium (II) from simulated wastewater by ion flotation technique, Iran. J. Environ. Health Sci. Eng., 10 (2013) 1–5.

[13] S. Bayar, A. Erdem Yilmaz, R. Boncukcuoğlu, B. Ali Fil, M. Muhtar Kocakerìm, Effects of operational parameters on cadmium removal from aqueous solutions by electrochemical coagulation, Desal. Water Treat., 51 (2013) 2635–2643.

[14] F. Fu, Q. Wang, Removal of heavy metal ions from wastewaters: A review, J. Environ. Manag., 92 (2011) 407–418.

[15] A. Hosseini-Bandegharaei, A. Allahabadi, A. Rahmani-Sani, A. Rastegar, R. Khamirchi, M. Mehrpouyan, R. Hekmat-Shoar, Z. Pajohankia, Thorium removal from weakly acidic solutions using titan yellow-impregnated XAD-7resin beads: kinetics, equilibrium and thermodynamic studies, J. Radioanal. Nucl. Chem., 309 (2016) 761–776.

[16] A. Hassoon Ali, Comparative study on removal of cadmium(II) from simulated wastewater by adsorption onto GAC, DB, and PR, Desal. Water Treat., 51 (2015) 5547–5558.

[17] N. Feng, X. Guo, S. Liang, Adsorption study of copper (II) by chemically modified orange peel, J. Hazard. Mater., 164 (2009) 1286–1292.

[18] K. Rao, M. Mohapatra, S. Anand, P. Venkateswarlu, Review on cadmium removal from aqueous solutions, Intern. J. Eng. Sci. Technol., 2 (2010) 81–103.

[19] S.E. Bailey, T.J. Olin, R.M. Bricka, D.D. Adrian, A review of potentially low-cost sorbents for heavy metals, Water Res., 33 (1999) 2469–2479.

[20] A. Saeed, M.W. Akhter, M. Iqbal, Removal and recovery of heavy metals from aqueous solution using papaya wood as a new biosorbent, Sep. Purif. Technol., 45 (2005) 25–31.

[21] M.H. Ehrampoush, H. Masoudi, A.H. Mahvi, M.H. Salmani, Prevalent kinetic model for Cd (II) adsorption from aqueous solutions on barley straw, Fresen. Environ. Bull., 22 (2013) 2314–2318.

[22] Y. Ding, D. Jing, H. Gong, L. Zhou, X. Yang, Biosorption of aquatic cadmium (II) by unmodified rice straw, Bioresour. Technol., 114 (2012) 20–25.

[23] O. Amuda, A. Giwa, I. Bello, Removal of heavy metal from industrial wastewater using modified activated coconut shell carbon, Biochem. Eng. J., 36 (2007) 174–181.

[24] U. Farooq, J.A. Kozinski, M.A. Khan, M. Athar, Biosorption of heavy metal ions using wheat based biosorbents–a review of the recent literature, Bioresour. Technol., 101 (2010) 5043–5053.

[25] A. Alahabadi, Z. Rezai, A. Rahmani-Sani, A. Rastegar, A. Hosseini-Bandegharaei, A. Gholizadeh, Efficacy evaluation of NH_4Cl induced activated carbon in removal of aniline from aqueous solutions and comparing its performance with commercial activated carbon, Desal. Water Treat., 57 (2016) 23779–23789.

[26] G. Moussavi, H. Hosseini, A. Alahabadi, The investigation of diazinon pesticide removal from contaminated water by adsorption onto NH_4Cl-induced activated carbon, Chem. Eng. J., 214 (2013) 172–179.

[27] M. Farasati, S. Haghighi, S. Boroun, Cd removal from aqueous solution using agricultural wastes, Desal. Water Treat., 57 (2016) 11162–11172.

[28] S. Gueu, B. Yao, K. Adouby, G. Ado, Kinetics and thermodynamics study of lead adsorption on to activated carbons from coconut and seed hull of the palm tree, Intern. J. Environ. Sci. Technol., 4 (2007) 11–17.

[29] J. Shah, M. Rasul Jan, M. Khan, S. Amir, Removal and recovery of cadmium from aqueous solutions using magnetic nanoparticle-modified sawdust: kinetics and adsorption isotherm studies, Desal. Water Treat., 57 (2016) 9736–9744.

[30] J. Shah, M. Rasul Jan, Atta ul Haq, M. Zeeshan, Equilibrium, kinetic and thermodynamic studies for sorption of Ni (II) from aqueous solution using formaldehyde treated waste tea leaves, J. Saudi Chem. Soc., 19 (2015) 301–310.

[31] J. Shah, M. Rasul Jan, Atta ul Haq, Removal of lead from aqueous media using carbonized and acid treated orange peel, Tenside Surfact. Det, 51 (2014) 240–246.

[32] Y. Shen, J. Tang, Z. Nie, Y. Wang, Y. Ren, L. Zuo, Preparation and application of magnetic Fe_3O_4 nanoparticles for wastewater purification, Sep. Purif. Technol., 68 (2009) 312–319.

[33] J. Shah, M. Rasul Jan, S. Jamil, Atta ul Haq, Magnetic particles precipitated onto wheat husk for removal of methyl blue from aqueous solution, Toxicol. Environ. Chem., 96 (2014) 218–226.

[34] P. Panneerselvam, N. Morad, K.A. Tan, Magnetic nanoparticle (Fe_3O_4) impregnated onto tea waste for the removal of nickel (II) from aqueous solution, J. Hazard. Mater., 186 (2011) 160–168.

[35] X. Li, Y. Tang, X. Cao, D. Lu, F. Luo, W. Shao, Preparation and evaluation of orange peel cellulose adsorbents for effective removal of cadmium, zinc, cobalt and nickel Colloids Surf. A: Physicochem. Eng. Asp., 317 (2008) 512–521.

[36] B.K. Biswas, K. Inoue, K.N. Ghimire, S. Ohta, H. Harada, K. Ohto, H. Kawakita, The adsorption of phosphate from an aquatic environment using metal-loaded orange waste, J. Colloid Interf. Sci., 312 (2007) 214–223.

[37] V. Gupta, A. Nayak, Cadmium removal and recovery from aqueous solutions by novel adsorbents prepared from orange peel and Fe_2O_3 nanoparticles, Chem. Eng. J., 180 (2012) 81–90.

[38] L.S. De Lima, M.D.M. Araujo, S.P. Quináia, D.W. Migliorine, J.R. Garcia, Adsorption modeling of Cr, Cd and Cu on activated carbon of different origins by using fractional factorial design, Chem. Eng. J., 166 (2011) 881–889.

[39] R. Gnanasambandam, A. Protor, Determination of pectin degree of esterification by diffuse reflectance Fourier transform infrared spectroscopy, Food Chem., 68 (2000) 327–332.

[40] S. Hashemian, K. Salari, Z. Atashi Yazdi, Preparation of activated carbon from agricultural wastes (almond shell and orange peel) for adsorption of 2-pic from aqueous solution, J. Ind. Eng. Chem., 20 (2014) 1892–1900.

[41] D.C. Montgomery, Design and analysis of experiments, John Wiley & Sons, 2008.
[42] S.L. Ahnazarova, V.V. Kafarov, V.M. Mackovskij, A.P. Rep'ev, Experiment optimization in chemistry and chemical engineering, Mir Publishers, 1982.
[43] Y. Safa, H.N. Bhatti, Adsorptive removal of direct textile dyes by low cost agricultural waste: Application of factorial design analysis, Chem. Eng. J., 167 (2011) 35–41.
[44] Y.B. Onundi, A. Mamun, M. Al Khatib, Y.M. Ahmed, Adsorption of copper, nickel and lead ions from synthetic semiconductor industrial wastewater by palm shell activated carbon, Intern. J. Environ. Sci. Technol., 7 (2010) 751–758.
[45] D. Ryan, J. Dean, R. Cassidy, Cadmium species in basic solution, Can. J. Chem., 43 (1965) 999–1003.
[46] C. Appel, L. Ma, Concentration, pH, and surface charge effects on cadmium and lead sorption in three tropical soils, J. Environ. Qual., 31 (2002) 581–589.
[47] K. Kadirvelu, C. Namasivayam, Activated carbon from coconut coirpith as metal adsorbent: adsorption of Cd (II) from aqueous solution, Adv. Environ. Res., 7 (2003) 471–478.
[48] M.R. Hartono, A. Assaf, G. Thouand, A. Kushmaro, X. Chen, R.S. Marks, Use of bamboo powder waste for removal of Bisphenol A in aqueous solution, Water Air Soil Poll., 226 (2015) 382.
[49] A. Hosseini-Bandegharaei, A. Alahabadi, A. Rahmani-Sani, A. Rastegar, R. Khamirchi, M. Mehrpouyan, J. Agah, Z. Pajohankia, Effect of nitrate and amine functionalization on the adsorption properties of a macroporous resin towards tetracycline antibiotic, J. Taiwan Inst. Chem. E., 66 (2016) 143–153.
[50] I. Langmuir, The constitution and fundamental properties of solids and liquids, J. Am. Chem. Soc., 38 (1916) 2221–2295.
[51] H. Freundlich, Adsorption in solution, Phys. Chem. Soc., 40 (1906) 1361–1368.
[52] S. Lagergren, B.K. Svenska, Zur theorie der sogenannten adsorption geloester stoffe, Veternskapsakad Handlingar, 24 (1898) 1–39.
[53] Y.S. Ho, J.C.Y. Ng, G. McKay, Kinetics of pollutant sorption by biosorbents: Review, Separ. Purif. Method, 29 (2000)189–232.
[54] W.J. Weber, J.C. Morris, Kinetics of adsorption on carbon from solution, J. Sanit. Eng. Div. Am. Soc. Civ. Eng., 89 (1963) 31–60.
[55] S.K. Milonjic, A consideration of the correct calculation of thermodynamic parameters of adsorption, J. Serb. Chem. Soc., 72 (2007) 1363–1367.
[56] A. Rahmani-Sani, R.R. Shan, L.G. Yan, A. Hosseini-Bandegharaei, Response to "Letter to Editor: Minor correction to the thermodynamic calculation using the distribution constant by Shan et al. and Rahmani-Sani et al.", J. Hazard. Mater., 325 (2017) 367–368.
[57] A. Alahabadi, A. Hosseini-Bandegharaei, G. Moussavi, B. Amin, A. Rastegar, H. Karimi-Sani, M. Fattahi, M. Miri, Comparing adsorption properties of NH_4Cl-modified activated carbon towards chlortetracycline antibiotic with those of commercial activated carbon, J. Mol. Liq., 232 (2017) 367–381.
[58] Y. Liu, Is the free energy change of adsorption correctly calculated?, J. Chem. Eng. Data, 54 (2009) 1981–1985.
[59] H.N. Tran, S.-J. You, A. Hosseini-Bandegharaei, H.-P. Chao, Mistakes and inconsistencies regarding adsorption of contaminants from aqueous solutions: A critical review, Water Res., 120 (2017) 88–116.